

<https://doi.org/10.1038/s41523-025-00818-8>

Breast cancer Intraoperative Margin Assessment using specimen PET-CT (BIMAP)

Check for updates

Anne-Sofie De Crem^{1,2} , Philippe Tummers^{1,3,4}, Herman Depypere^{1,3,4}, Geert Braems^{1,3,4}, Rawand Salihi^{1,4}, Glenn Vergauwen^{1,4}, Giovanni Cisternino⁵, Koen Van de Vijver^{4,6,7}, Pieter De Visschere^{4,7,8}, Kathia De Man^{7,8}, Bliese Van den Broeck⁸, Sigi Hendrickx⁸, Liv Veldeman^{3,4,9}, Christel Monten^{3,4,9}, Jens M Debacker^{10,11}, Hannelore Denys^{2,4,12} & Menekse Göker^{1,2,4}

Positive surgical margins in breast-conserving surgery (BCS) for breast cancer occur in 20% of cases, making intraoperative margin assessment (IMA) crucial to avoid re-operations. This study evaluated specimen PET-CT imaging for IMA in 41 patients undergoing BCS. Specimen PET-CT imaging was performed with the β -CUBE/X-CUBE (MOLECUBES) or the AURA 10 (XEOS). Seven physicians, with varying experience, assessed margin status postoperatively as positive, close (≤ 1 mm), or negative using PET-CT images at 10 min acquisition time and low reconstructed [^{18}F]FDG dose (0.8MBq/kg). Close margins on PET-CT were analyzed once as positive and once as negative. Histopathology was the gold standard. The proposed technique showed 91% sensitivity and 86% specificity for invasive ductal carcinoma (IDC). Histopathology identified 9 positive margins in 31 IDC cases; 88% were detected by all physicians on specimen PET-CT whereas standard of care identified 44%. Therefore, specimen PET-CT will improve IMA in BCS and potentially reduce re-operation rates. The trial is registered since 20/01/2020 on ClinicalTrials.gov (ID: NCT04343079) with the title: "Intra-operative PET-CT: a Novel Approach to Determine Excision Margins in Lumpectomy Breast Cancer".

The standard treatment for early-stage breast cancer (BC) typically involves breast-conserving surgery (BCS) and a sentinel node procedure followed by radiation therapy. This approach offers better cosmetic outcomes, improved quality of life, and comparable survival rates (both overall survival and disease-free survival) compared to total mastectomy¹⁻³. However, local recurrence (LR) rates after BCS range from 3.5% to 6.5% after 10 years⁴. The most significant risk factor for LR is a positive resection margin^{1,5,6}, as LR usually occurs at the previous excision site and shares the same histology as the primary tumor⁷. According to recent ESMO guidelines⁸, positive margins are defined as ink on tumor for invasive cancers or a tumor-free margin of <2 mm for ductal carcinoma in situ (DCIS).

Even in experienced hands, positive excision margins for invasive BC are found in approximately 20% (9% to 36%) of BCS cases at international

breast care units⁹, and are associated with significantly higher LR rates, i.e., 27% for positive margins versus 7% for negative margins¹⁰. Consequently, a re-operation is recommended when tumor free margins are not achieved. Until now, literature still reports a high re-operation rate of 14%¹¹. Re-operations have been associated with higher risk of surgical complications, poorer cosmetic outcomes, delay in the administration of adjuvant therapy, and increased psychological and economic burdens for patients and society^{12,13}.

To avoid re-operations due to positive margins, a rapid and reliable method for intraoperative margin assessment (IMA) is needed. Traditionally, specimen radiography for non-palpable masses is used as the standard of care (SOC) IMA method but other techniques have been reported, including frozen section, intraoperative ultrasound, and micro-CT. The

¹Department of Obstetrics and Gynecology, Ghent University Hospital, Ghent, Belgium. ²Faculty of Medicine and Health Science, Ghent University, Ghent, Belgium. ³Department of Human Structure and Repair, Ghent University, Ghent, Belgium. ⁴Cancer Research Institute Ghent, Ghent, Belgium. ⁵Breast Surgery Unit, IRCCS San Raffaele Scientific Institute, Milan, Italy. ⁶Department of Pathology, Ghent University Hospital, Ghent, Belgium. ⁷Department of Diagnostic Sciences, Ghent University, Ghent, Belgium. ⁸Department of Radiology and Nuclear Medicine, Ghent University Hospital, Ghent, Belgium. ⁹Department of Radiation Oncology, Ghent University Hospital, Ghent, Belgium. ¹⁰Molecular Imaging and Therapy research group, Vrije Universiteit Brussel, Brussels, Belgium. ¹¹Department of Nuclear Medicine, University Hospital Brussels, Brussels, Belgium. ¹²Department of Medical Oncology, Ghent University Hospital, Ghent, Belgium. e-mail: anne-sofie.de.crem@hotmail.com; menekse.goker@uzgent.be



performance of these methods has been reviewed in recent meta-analyses^{14,15}. However, no current method offers high diagnostic performance in combination with minimal disruption to the surgical workflow.

Here, we used a novel IMA technique: high-resolution Positron Emission Tomography - Computed Tomography (PET-CT) specimen imaging with the use of ¹⁸F-fluoro-deoxyglucose ([¹⁸F]FDG). This method combines the high sensitivity of PET for detecting metabolically active tumor tissue and the precise anatomical delineation of CT. This clinical open-label, prospective single-arm study builds on a pilot study that explored the feasibility of this new IMA technique¹⁶. In the pilot study ($n = 20$), images were analyzed by three physicians and compared to final histopathology, which is considered the gold standard.

The primary aim of this study is to (1) assess the diagnostic performance of specimen PET-CT as an IMA technique by comparing it to final histopathology in the largest patient cohort until now, involving multiple evaluating physicians. Additionally, the study aims to (2) determine its clinical value by comparing it to the SOC (i.e., specimen radiography for non-palpable specimens) and other established IMA methods. Further analyses examine the influence of physician experience and confidence levels. In short, the objective is to demonstrate the diagnostic performance and clinical value of specimen PET-CT, providing a foundation for further research that could support its clinical implementation.

Results

Descriptives

Between June 2017 and December 2022, 49 patients were enrolled in this study, for which 41 cases were analyzed. A detailed overview of the 8 cases that were unsuitable for interpretation, e.g., no tumor present in specimen after NACT (neoadjuvant chemotherapy), can be found in the supplementary Table 1. An inclusion stop was seen during the covid pandemic. The following patients were included: 31 patients with IDC (with or without DCIS), 2 patients with DCIS-only, 6 patients with ILC (with or without lobular carcinoma in situ (LCIS)), and 2 patients who had undergone NACT (both also IDC cases). Patient and tumor characteristics are detailed in Table 1. In 25 patients, the tumor was not palpable thus a guidewire was placed and specimen radiography was performed as part of SOC.

Image quality

A region of high [¹⁸F]FDG uptake was visualized in every resected specimen across all anatomical planes, in correlation with the histopathology findings, for all types of tumor. An example of the specimen PET-CT images is shown in Fig. 1 for an IDC case and Fig. 2 for an DCIS case. Visual comparison of the PET-CT images corresponding to the received dose (4 MBq/kg for $n = 40$ patients) and to the reconstructed dose of 0.8 MBq/kg with 10 min acquisition time, showed similar uptake patterns (see Supplementary Fig. 1). Therefore, all images were interpreted by the physicians at this low dose and short acquisition time. Both scanners (MOLECUBES and AURA10), differing mainly in usability, offered again similar image quality (which was already established in the pilot study), thus images from both scanners were used for the same analysis.

The mean time between [¹⁸F]FDG injection and PET-CT image acquisition was 185 minutes (range: 47–351 min) and the mean injected dose was 288 MBq (range: 58–417 MBq). For uniformity and to mimic the intraoperative settings, the radioactivity of the excised specimen was recalculated at the mean time of PET acquisition, i.e., 185 min post-injection. The median radioactivity at 185 min post-injection was 75.5 kBq for a 4 MBq/kg dose and 15.1 kBq for a 0.8 MBq/kg dose (median was used due to outlier behavior). For an overview, see Supplementary Table 2.

Margin analysis

The mean sensitivity and specificity, categorized by level of experience and type of BC, are presented in Table 2. In the IDC group ($n = 31$), a mean overall sensitivity of 75% and specificity of 94% were observed when close = neg. More importantly, these values altered to 91% and 86% respectively, when close = pos. Within the IDC group, specificity decreased

Table 1 | Overview of patient and tumor characteristics

Category	Subcategory	Patients ($n = 41$)
Age mean [min-max] (years)		60 [38–81]
Length mean [min-max] (cm)		164.1 [150–178]
Weight (mean [min-max]) (kg)		70.8 (53–103)
Clinical stage (n (%))	Tis	2 (5%)
	T1a (≤ 5 mm)	2 (5%)
	T1b (≤ 10 mm)	10 (24%)
	T1c (≤ 20 mm)	19 (46%)
	T2 (≤ 50 mm)	8 (20%)
	N0	34 (83%)
	N1a	5 (12%)
	N2a	2 (5%)
Tumor Histology (n (%))	IDC	31 (75%)
	ILC	6 (15%)
	DCIS	2 (5%)
	NACT	2 (5%)
Nothingham Grade (n (%))	1	9 (22%)
	2	20 (48%)
	3	11 (27%)
	N/A	1 (3%)
Estrogen receptor (n (%))	Negative	3 (7%)
	Positive	37 (90%)
	N/A	1 (3%)
Progesterone receptor (n (%))	Negative	9 (22%)
	Positive	31 (75%)
	N/A	1 (3%)
HER2 amplification (n (%))	Negative	31 (75%)
	Positive	6 (15%)
	N/A	4 (10%)
Ki-67 classification (n (%))	High ($> 15\%$)	17 (41%)
	Medium (10–15%)	7 (17%)
	low ($< 10\%$)	15 (37%)
	N/A	2 (5%)

Tumors were divided into four groups: IDC invasive ductal carcinoma, ILC invasive lobular carcinoma, DCIS ductal carcinoma in-situ only, and NACT neoadjuvant chemotherapy. N/A stands for not available.

limited across all levels of experience, while sensitivity increased when shifting from close = neg to close = pos i.e., from 74% to 89% for the experienced group, from 70% to 92% for the limited experience group, and was 89% for both scenarios in the no experience group. This trend holds across all levels of experience and types of BC, except in the DCIS group, where specificity remained constant. Important to note is the small sample size for other tumor types. DCIS only cases ($n = 2$) showed a very high sensitivity and specificity of 100% (if close = pos), whereas patients with ILC ($n = 6$) and NACT ($n = 2$) showed lower sensitivity (50% and 43% resp.) and specificity (54% and 43% resp.). Comparing experience levels in the IDC (close = pos) group, sensitivity differed by just 3%, and specificity varied by 14%, see Table 2.

IDC cases

Positive margins of IDC on histopathology were observed in 29% (9/31) of cases, as shown in Table 3. In this study, specimen PET-CT was performed intraoperatively and retrospectively analyzed. Had PET-CT results been

Fig. 1 | Example of a specimen PET-CT and CT only image in an IDC case. The window is set to 80%. Final histopathology showed a 2 mm posterior positive margin. All seven physicians assessed these margins as positive (post-operatively). Re-operation was needed. Surgical orientation is shown for each plane (i.e., transverse, coronal, and sagittal): “ant” is anterior, “pos” is posterior, “inf” is inferior, “sup” is superior, “lat” is lateral, “med” is medial.

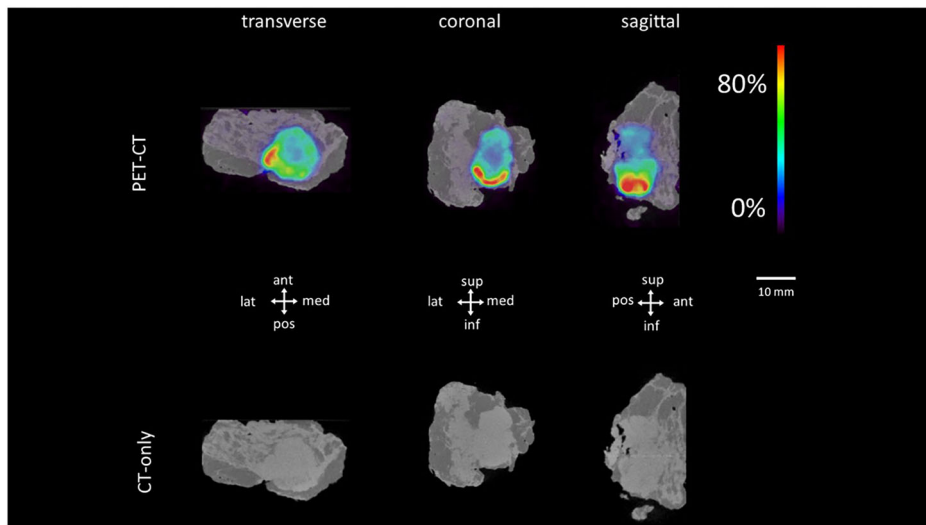


Fig. 2 | Example of a specimen PET-CT and CT only image in a DCIS case. The window is set relative to 50%. The guide wire is visible as well. Final histopathology showed a medial positive margin. All seven physicians assessed the image as positive (post-operatively).

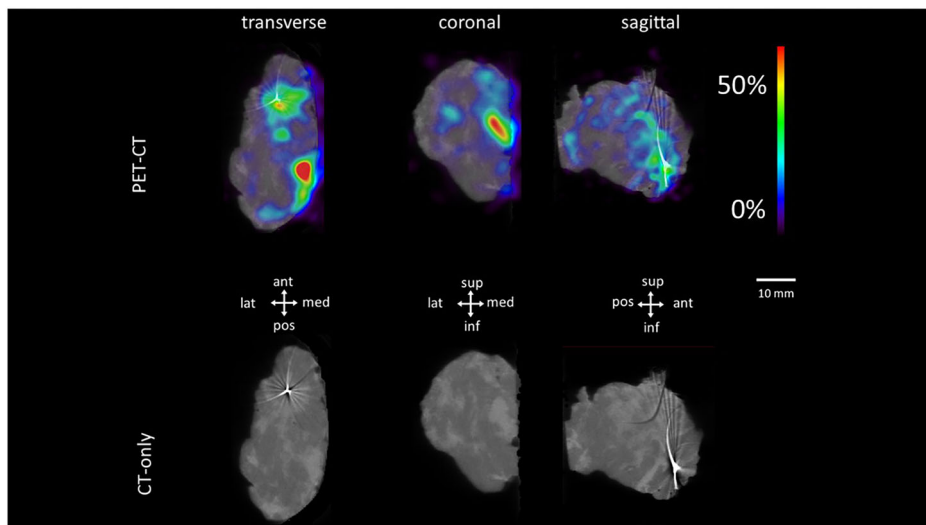


Table 2 | Overview of calculated sensitivity and specificity percentages

Assessor group	Close margin classification	IDC (n = 31)		ILC (n = 6)		DCIS (n = 2)		NACT (n = 2)	
		sens	spec	sens	spec	sens	spec	sens	spec
OVERALL	close = neg	75	94	50	86	86	100	29	71
	close = pos	91	86	50	54	100	100	43	43
Experienced (n = 3)	close = neg	74	95	50	83	66	100	0	100
	close = pos	89	91	50	58	100	100	33	33
Limited experience (n = 3)	close = neg	70	95	50	92	100	100	33	66
	close = pos	92	85	50	58	100	100	33	66
No experience (n = 1)	close = neg	89	86	50	75	100	100	100	0
	close = pos	89	77	50	25	100	100	100	0

Calculated for all groups (IDC, ILC, DCIS only and NACT), by level of experience (experienced, limited experience and no experience) and by analyzing the “close margins” once as a positive margin (close = pos) and once as a negative margin (close = neg). The overall sensitivity (sens) and specificity (spec) percentages were given as well. The experienced group consisted of two nuclearist and one radiologist. The limited experience group of three breast surgeons and the one identified as “no experience”, was a resident in gynecology.

Table 3 | Overview of IDC cases (n = 31)

Positive margins		
Histopathology (gold standard)	9/31 (29%)	
Specimen PET-CT when all physicians (7/7) would perform a cavity shave	8/9 (89%)	
Compared with no IMA technique	NNT of 4 (26%, ARR 8/31)	
Compared with SOC	NNT of 8 (13%, ARR 4/31)	
Interventions (in case of positive margins)		
Direct cavity shave (SOC)	3/9 (33%)	2 seen on PET-CT
Re-operation not possible (skin)	1/9 (11%)	all seen on PET-CT
Re-operation needed	5/9 (55%)	all seen on PET-CT

The absolute risk reduction (ARR) and the number needed to treat (NNT) of the specimen PET-CT as IMA technique was calculated, once in comparison with no intervention, and once in comparison with SOC. The interventions that were done in case of positive margins, were described

available in real-time for surgical decision-making, they could have supported cavity shave recommendations in 8 of these 9 positive margin cases, potentially reducing the positive margins to just 1 in 31. The one margin not detected on PET-CT, had a cavity shave according to SOC. This represents an absolute risk reduction (ARR) of 0.26 (8/31) when comparing PET-CT to no IMA technique, resulting in a Number Needed to Treat (NNT) of 4. When comparing PET-CT to the SOC (specimen radiography with a guide wire for non-palpable lesions), specimen PET-CT again showed advantages: the ARR was 0.13 (4/31, as 5 of 31 positive margins were missed with SOC, compared to 1 of 31 with PET-CT), yielding a NNT of 8. Out of 9 patients with positive margins, 3 received an immediate cavity shave based on specimen radiography (SOC). In one case, re-operation was not possible since the positive margin was located at the skin side. Consequently, 5/9 (55%) patients still required a re-operation under standard care. Importantly, all seven physicians recommended a cavity shave supported by the specimen PET-CT images, in all 5 cases. Over a mean follow-up period of 49 months (19–79 months), one recurrence in the IDC group was seen (1/31 or 3%).

Confidence level

Confidence levels were analyzed across various parameters, with detailed findings presented in Supplementary Table 3. Notably, the average rate of confident interpretations for IDC cases was 76%. Furthermore, when surgeons interpreted the images as close, this was generally associated with a low confidence level, i.e., 19% confident, 57% limited confident, and 24% not confident. In these 'close' cases, cavity shaves were suggested by the surgeons in the majority (80%) of instances.

Discussion

This study evaluated the diagnostic performance and clinical value of specimen PET-CT imaging for IMA in patients undergoing BCS.

With a sensitivity of 91% and a specificity of 86%, specimen PET-CT accurately defined the margins in IDC tumors, the most common form of BC, representing 75.2% of all BC cases in Belgium¹⁷. Additionally, the sensitivity improved when close = pos, indicating an increased detection of true positive margins (positive margins that would be missed otherwise), thereby reducing the need for re-operation by enabling immediate cavity shaving. Encouragingly, specificity decreased only limited when close = pos, suggesting minimal additional false positives thus minimal excessive tissue removal, maintaining comparable cosmetic outcomes. This implies that identifying a close margin on specimen PET-CT as positive is advantageous: performing a cavity shave in these cases could prevent re-operation without compromising cosmetic results. Importantly, for these close margins, most surgeons opted for a cavity shave, likely due to the belief that avoiding re-operation outweighs removing extra tissue. Unfortunately, due to the low number of patients in other subgroups (ILC, DCIS, and NACT), interpreting these results is

challenging, and no definitive conclusions can be made. Nevertheless, the promising sensitivity and specificity of 100% in DCIS (n = 2) cases, suggests its diagnostic performance in this subgroup as well.

The detailed analysis of the positive margins seen in the IDC cases, highlights the clinical value of specimen PET-CT imaging: out of 31 IDC cases, 9 had positive margins on final histopathology. With specimen PET-CT guidance, surgeons recommended cavity shaves in 8 of these 9 cases, resulting in a very low NNT of 4. This means that scanning 4 patients with specimen PET-CT and performing a cavity shave when indicated, could prevent one positive margin on final histopathology and thus avoid one re-operation. When comparing specimen PET-CT to the SOC (specimen radiography with a guide wire for non-palpable lesions), also a low NNT of 8 was found. This indicates that for every 8 patients scanned with specimen PET-CT, one positive margin (and potentially a re-operation) could be avoided compared to SOC. These findings show the clinical value of PET-CT in reducing positive margins and support further research to explore its broader use in BCS. Most importantly, in all 5 cases that needed a re-operation, all seven physicians recommended a cavity shave supported by the specimen PET-CT images. If this device was used intra-operatively, all re-operations could have been avoided.

The safety and minimal workflow interruption of this technique are supported by the clear visualization of high [18 F]FDG uptake in every resected specimen, even with a 10-minute acquisition time and a reconstructed dose as low as 0.8 MBq/kg. Since the sentinel lymph node (SLN) procedure can be performed during this 10-min scanning time, there is almost no interruption in the surgical flow. Second, the median activity for this 0.8 MBq/kg dose was only 15.1 kBq, indicating limited radiation exposure for the surgical team and histopathologist. Rep et al.¹⁸ showed that even with a specimen activity of 333 kBq (i.e., 5 µSv/h at 10 cm of the specimen), the dose rate was below the IEC safety performance standard. Additionally, a recent study by Lambert et al. investigated the practical aspects of implementing a safe workflow for intraoperative PET-CT imaging¹⁹. The authors monitored radiation dose rates around the patient throughout the procedure and recorded absorbed doses for all involved personnel, including surgeons and instrumenting nurses. With a normalized injected activity of 1 MBq/kg, the estimated median absorbed dose per procedure was 15.6 µSv for surgeons and 14.1 µSv for instrumenting nurses. The study concluded that the 1 MBq/kg dose level provided high-quality imaging while enabling a safe and feasible clinical implementation. Although some radiation exposure is inherent to the procedure, reducing the injected dose to 0.8 MBq/kg—which is approximately one-fifth of a standard whole-body PET-CT dose—further minimizes exposure, keeping it within safe limits. Consequently, this method is safe and no changes to the standard workflow, such as use of lead containers, are necessary. Third, comparison of physician experience levels in the IDC group (close = pos) revealed only a 3% difference in sensitivity, suggesting that even inexperienced physicians can achieve high diagnostic performance after interpretation training. This indicates the ease of implementation for the interpretation flowchart. Additionally, the confident level for IDC cases was consistently around 76%, reflecting both the clarity of PET-CT images and the effectiveness of the interpretation guidelines. However, confidence levels for DCIS, ILC, and NACT cases were lower, indicating that the guidelines may need adaptation for these subtypes, though the small sample size limits definitive conclusions. In summary, this technique is safe, straightforward to implement, and minimally disruptive to the surgical workflow.

Recent large-scale systematic reviews highlight the sensitivity and specificity of other IMA techniques: ultrasound (72% and 78%), frozen section (81% and 97%), and specimen radiography (52% and 77%)^{15,18}. Although frozen section has traditionally been the IMA gold standard, its use is limited in many hospitals due to many challenges: it requires a pathologist on standby, allows only spot checks, involves complex transport logistics, and averages 24.7 minutes (range 10–50 min), causing workflow delays. Additionally, it can damage specimen margins, interfering with final histopathology^{20,21}. Frozen section re-operation rates are 5.9% (range: 0–23.9%), with a local recurrence (LR) rate of 4.2% over 12–62 months of

follow-up²², making it the benchmark for less disruptive IMA techniques. Ultrasound, identified as the most accurate method by Manhoobi et al.¹⁵ is often impractical because it requires an in-room breast radiologist, interrupting workflow and adding resource demands. It is also operator-dependent, less effective for DCIS detection, and susceptible to the “pancake phenomenon,” which can lead to false positives²³. Consequently, it falls short as a reliable alternative to frozen section¹⁵. Other techniques discussed in Armani et al., are promising but not yet clinically practical or proven to reduce re-operation rates. These include optical coherence tomography, ClearEdge, MarginProbe, micro-CT, imprint cytology, fluorescent imaging (LUM015), and cavity margins²⁴. Integration of artificial intelligence, such as CAMELYON16 for pathology, shows potential but requires further validation²⁴. In short, according to literature, no current IMA technique can provide diagnostic performance together with a minimal interruption of the surgical flow. For this reason, the relatively high sensitivity and specificity of specimen PET-CT (91% and 86% for IDC), its clinical value and its minimal interruption in the surgical flow, shows the potential of this new technique to become a new SOC IMA method.

The primary challenge identified in this study is the accurate margin assessment for DCIS, ILC, and NACT cases, where the limited patient numbers hinder robust conclusions. Additionally, different uptake patterns in DCIS, ILC, and NACT cases imply the need for an adapted window setting, and so suggest adjustments to the interpretation flow. Here, only the invasive tumor mass was analyzed in both IDC and ILC cases, leaving any in-situ components unassessed. Therefore, future research should focus on training physicians to assess these in-situ components within invasive carcinomas as well.

Another challenge is the potential interference of [¹⁸F]FDG activity with SLN localization using the gamma probe to detect [^{99m}Tc]Tc-nanocolloid. Improved results were observed with the 1-day protocol and use of patent blue. Future studies might also benefit from adjusting gamma probe settings to mitigate this issue. Although radiation exposure to staff and patients is limited (only 1/5 of a full body PET-CT dose is used), other IMA techniques, such as frozen section, offer zero or significantly lower radiation exposure. Device cost is another consideration, its justification hinges on cost-effectiveness analysis and prevention of re-operations.

Important to note is that the potential of specimen PET-CT imaging extends beyond BC, with promising results observed in head-and-neck cancer²⁵, prostate cancer²⁶, thyroid cancer¹⁹ and more. Therefore, this multidisciplinary view can change the cost-effectiveness analysis drastically. In these studies, the use of different tracers, such as [¹⁸F]PSMA and [⁶⁸Ga]PSMA for specimen PET-CT imaging in prostate cancer, and [¹⁸F]Choline for parathyroid imaging was demonstrated^{19,27}. For breast cancer, the emergence of novel PET tracers may offer added value in future research. As estrogen receptor (ER)-positive breast cancer is the most prevalent subtype, [¹⁸F]FES PET imaging—which allows visualization and quantification of ER expression across all tumor sites—presents a promising avenue for future studies²⁸.

In conclusion, the findings of this study are promising, indicating that this novel IMA technique achieves high diagnostic performance in margin assessment and offers valuable support for BCS. To confirm these findings, a multicentric study (BrIMA) with a larger patient cohort for all subtypes, is ongoing.

Methods

Ethics and patient information

The study was conducted in compliance with local and national regulations and in accordance with the Declaration of Helsinki and the International Council for Harmonisation Guidelines for Good Clinical Practice. The study protocol and amendments were approved by an independent ethics committee or review board at the participating institution (Ghent University Hospital Ethics Committee, identifier EC/2017/0200); all patients provided written informed consent. The trial is registered since 20/01/2020 on ClinicalTrials.gov (ID: NCT04343079) with the title: “Intra-operative

PET-CT: A Novel Approach to Determine Excision Margins in Lumpectomy Breast Cancer”.

Eligible participants were females aged 18 years or older, diagnosed with early-stage invasive BC (T1-2, N0-1, ductal or lobular), and scheduled for BCS. Exclusion criteria included pregnancy or lactation, diabetes, inflammatory BC, prior surgical treatment or radiotherapy of the affected breast, logistical infeasibility, i.e., appointment at the nuclear medicine department for radiotracer injection that would result in an unacceptable delay of surgery, and participation in other clinical trials. For an overview of these inclusion and exclusion criteria see Supplementary Table 4.

Surgical procedure with specimen PET-CT imaging

On the day of surgery, 40 patients received an intravenous administration of 4 MBq/kg of [¹⁸F]FDG, whereas only one patient received an intravenous administration of 0.8 MBq/kg of [¹⁸F]FDG. Those scheduled for SLN were given a single subcutaneous injection of 148 MBq of [^{99m}Tc]Tc-nanocolloid around the tumor, as part of the standard treatment. In case of non-palpable masses, a guide wire placement was done preoperatively.

Subsequently, BCS was performed. After excision, the radioactivity level of each specimen (in kBq) was measured with a VDC-404 dose calibrator (Veenstra Instruments, Joure, the Netherlands). Next, a high-resolution specimen PET-CT scan was performed. At the start of the study, only the preclinical MOLECUBES scanners (MOLECUBES, Ghent, Belgium) situated at the radiology department, were available (n = 35). A CT scan (X-CUBE) of approximately 3 min was performed, followed by a PET scan (β-CUBE) with an acquisition time between 20 (n = 1), 30 (n = 26), and 40 (n = 8) min. Later, the AURA 10 (XEOS, Ghent, Belgium) was used (n = 6), i.e., a mobile and compact PET-CT device designed specifically for intraoperative use with a scan time of around 10 min for PET and 1 min for CT. All images were reconstructed postoperatively to emulate an acquisition time of 10 min and a low [¹⁸F]FDG dose of 0.8 MBq/kg. This approach aimed to increase uniformity across the different acquisition parameters and to stimulate a potential future clinical protocol involving shorter PET acquisition time and lower radiotracer dose. The decision to reconstruct the images at a dose of 0.8 MBq/kg, was based on the results of Göker et al.¹⁶, which showed adequate image quality at this reconstruction parameter. Other reconstruction parameters are detailed in Supplementary Table 5.

During the specimen PET-CT imaging, the SLN procedure was conducted using a Neoprobe 2000 Gamma Detection System with an NPB14A 14 mm Bluetooth probe (Neoprobe Corporation, Dublin, OH). Throughout the study, interference with [¹⁸F]FDG activity was seen. The first twenty patients were injected with [^{99m}Tc]Tc-nanocolloid the day before the surgery (2-day protocol), leading to a higher overall signal at the time of surgery and the need for a periareolar subdermal injection of 2 ml Patent Blue (V sodium salt injection. Guerbet, Gorinchem, the Netherlands) to correctly locate the sentinel node. The remaining twenty-one patients were injected the same day of the surgery (1-day protocol) giving a better signal thus no Patent Blue was needed.

In this study, the PET-CT images were not assessed intraoperatively. After imaging of the tumor specimen by the PET-CT, it was brought either first to the radiology department to perform a specimen radiography (in case of a guide wire localization), or directly to the histopathology department. At the histopathology department, the tumor margins were assessed following ASCO/CAP protocols^{29,30}. Tumor size and resection margin status were microscopically measured. For each lamella of the resected specimen, presence or absence of in situ and/or invasive carcinoma was analyzed, along with its relation to the inked surgical resection margins. Final histopathology served as the gold standard for comparing the PET-CT results.

Image assessment

The PET-CT images were interpreted postoperatively by seven physicians, who were blinded to the patient and the histopathological

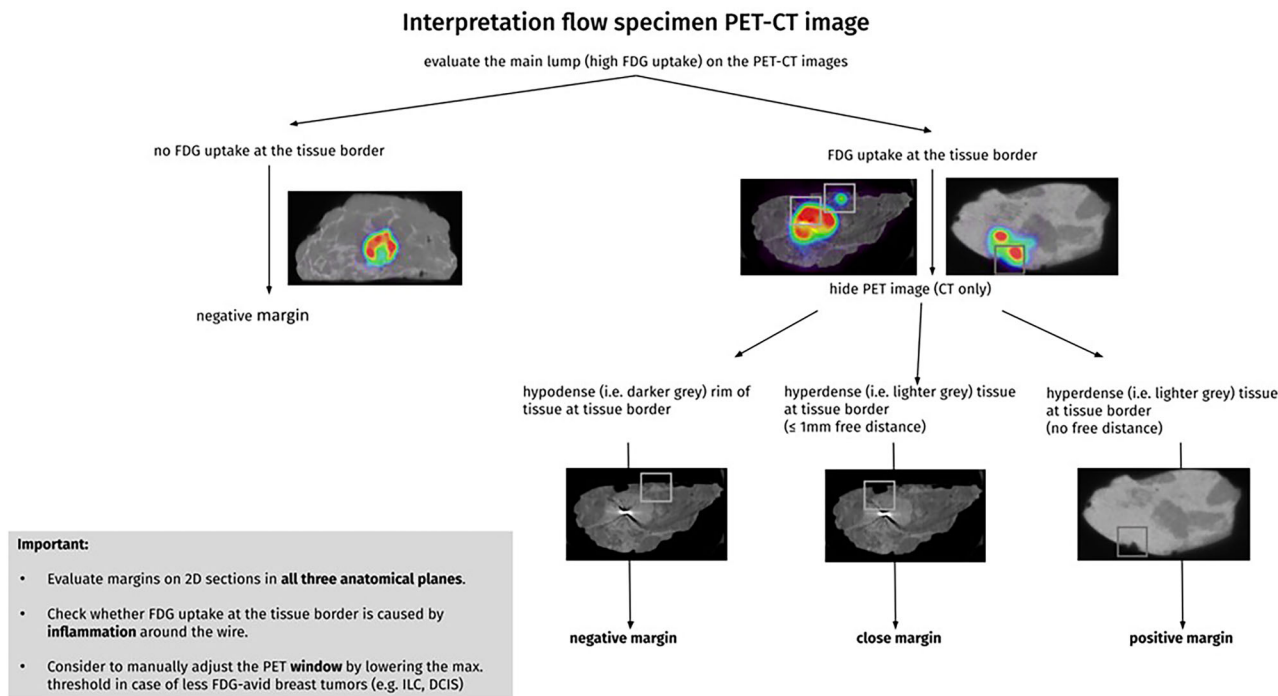


Fig. 3 | Interpretation workflow. Visualization of the interpretation workflow. In this study, margins were evaluated as negative, (>1 mm margin free of tumor), close (≤ 1 mm margin free of tumor), or positive (tumor seen on the specimen margins).

results. All physicians underwent interpretation training, which included: (1) learning the fundamentals of PET and CT, (2) training on interpreting specimen PET-CT images and assessing margins using an interpretation flow chart, and (3) practicing with test cases ($n = 10$) to verify their comprehension. Importantly, the image interpretation flow, illustrated in Fig. 3, guided the physicians in scoring the margin status of the PET-CT images. The training primarily focused on the main tumor lump, without specific evaluation for in-situ components in invasive cases. After the training, the physicians were asked to determine the margin status, i.e., positive ($= 0$ mm), close (≤ 1 mm), or negative (> 1 mm), for all six orientations (anterior, posterior, superior, inferior, medial and lateral) based on the PET-CT images. Here, a single definition of a positive margin, i.e., no free distance, is used in the interpretation flow, so no distinction is made between invasive and in-situ components.

The physicians also assessed their confidence in margin evaluation (1 = not confident, 2 = limited confidence, or 3 = confident), identified the orientation of the closest margin and indicated if they would take a cavity shave. The window setting (red means a high uptake, purple/blue a low uptake) is set to 80% to optimize contrast and signal intensity for most tumor types. For invasive lobular carcinoma and ductal carcinoma in-situ, it is reduced to 50% based on our pilot study, which showed that a narrower window enhances visualization of their subtle, diffuse growth pattern and improves margin delineation. All specimen PET-CT images were visualized using AMIDE (Amide's a Medical Image Data Examiner), an open-source software platform.

Statistics and image analysis

Descriptive statistics were used to detail patient and tumor characteristics. In the analysis, the physicians were divided into predetermined subgroups depending on experience level: (1) no experience, i.e., one resident in gynecology who only received the image interpretation training (A.D.C), (2) limited experience, i.e., three breast surgeons who already had experience with interpreting specimen PET-CT images for study purposes (G.V., M.G., G.C.), and (3) experienced, i.e., two nuclear medicine physicians (K.M., B.B.)

and one radiologist (P.V.) who have experience with PET and/or CT during their daily practice. All physicians work at Ghent University Hospital except for one breast surgeon from IRCCS San Raffaele Scientific Institute in Milan (Italy).

The sensitivity and specificity of the proposed method were calculated for each physician, using histopathology as the gold standard. Since the image interpretation focused on the main tumor lump, only invasive margins indicated by histopathology were included for invasive ductal carcinoma (IDC) and invasive lobular carcinoma (ILC) cases. Additionally, these metrics were determined based on varying levels of experience and different tumor types: IDC, ILC and ductal carcinoma in situ (DCIS), or a different treatment type: after neoadjuvant chemotherapy (NACT). The analysis included an evaluation of close margins in two ways: first, when margins analyzed as 'close' were considered 'positive' (close = pos), and second, when margins analyzed as 'close' were considered 'negative' (close = neg). Ultimately, this approach allowed us to simplify the close margin outcomes into a final dichotomous variable, distinguishing clearly between positive and negative results.

The level of confidence with respect to various types of tumors, the number of 'close' interpretations, and the number of cavity shaves that the physician 'would take' when a 'close' interpretation is made, were calculated as well. The activity of each specimen was recalculated to reflect the activity at 185 minutes post-injection, which is the average time between injection and PET acquisition. This was done for both 4 MBq/kg and 0.8 MBq/kg injection scenarios. Finally, the mean and median values of these recalculated activities were determined.

Data availability

The data supporting the findings of this study are available from the corresponding author upon reasonable request.

Received: 28 November 2024; Accepted: 14 August 2025;

Published online: 26 September 2025

References

1. Fisher, B. et al. Twenty-year follow-up of a randomized trial comparing total mastectomy, lumpectomy, and lumpectomy plus irradiation for the treatment of invasive breast cancer. *N. Engl. J. Med.* **347**, 1233–1241 (2002).
2. Poggi, M. M. et al. Eighteen-year results in the treatment of early breast carcinoma with mastectomy versus breast conservation therapy: the National Cancer Institute Randomized Trial. *Cancer* **98**, 697–702 (2003).
3. Veronesi, U. et al. Twenty-year follow-up of a randomized study comparing breast-conserving surgery with radical mastectomy for early breast cancer. *N. Engl. J. Med.* **347**, 1227–1232 (2002).
4. Anderson, S. J. et al. Prognosis after ipsilateral breast tumor recurrence and locoregional recurrences in patients treated by breast-conserving therapy in five National Surgical Adjuvant Breast and Bowel Projects protocols in node-negative breast cancer. *J. Clin. Oncol.* **27**, 2466–2473 (2009).
5. McCahill, L. E. et al. Variability in reexcision following breast conservation surgery. *JAMA* **307**, 467–475 (2012).
6. Waljee, J. F. et al. Predictors of re-excision among women undergoing breast-conserving surgery for cancer. *Ann. Surg. Oncol.* **15**, 1297–1303 (2008).
7. Scopa, C. D. et al. Evaluation of margin status in lumpectomy specimens and residual breast carcinoma. *Breast J.* **12**, 150–153 (2006).
8. Loibl, S. et al. Early breast cancer: ESMO clinical practice guideline for diagnosis, treatment, and follow-up. *Ann. Oncol.* **35**, 159–182 (2024).
9. Brouwer de Koning, S. G. et al. Tumor resection margin definitions in breast-conserving surgery: Systematic review and meta-analysis of the current literature. *Clin. Breast Cancer* **18**, e595–e600 (2018).
10. Park, C. C. et al. Outcome at 8 years after breast-conserving surgery and radiation therapy for invasive breast cancer: Influence of margin status and systemic therapy on local recurrence. *J. Clin. Oncol.* **18**, 1668–1675 (2000).
11. Havel, L. et al. Impact of the SSO-ASTRO margin guideline on rates of re-excision after lumpectomy for breast cancer: a meta-analysis. *Ann. Surg. Oncol.* **26**, 1238–1244 (2019).
12. Grant, Y. et al. Patient-level costs in margin re-excision for breast-conserving surgery. *Br. J. Surg.* **106**, 384–394 (2019).
13. Abe, S. E. et al. Margin re-excision and local recurrence in invasive breast cancer: A cost analysis using a decision tree model. *J. Surg. Oncol.* **112**, 443–448 (2015).
14. St John, E. R. et al. Diagnostic accuracy of intraoperative techniques for margin assessment in breast cancer surgery: A meta-analysis. *Ann. Surg.* **265**, 300–310 (2017).
15. Manhoobi, I. P. et al. Diagnostic accuracy of radiography, digital breast tomosynthesis, micro-CT and ultrasound for margin assessment during breast surgery: A systematic review and meta-analysis. *Acad. Radiol.* **29**, 1560–1572 (2022).
16. Göker, M. et al. 18F-FDG micro-PET/CT for intra-operative margin assessment during breast-conserving surgery. *Acta Chir. Belg.* **120**, 366–374 (2020).
17. van Walle, L. et al. Incidence of breast cancer subtypes in Belgium: a population-based study. *Belg. J. Med Oncol.* **14**, 263–273 (2020).
18. Rep, S., Santos, A. & Testanera, G. Radiation protection and dose optimisation—A technologist's guide. <https://doi.org/10.52717/CIGE6278> (2016).
19. Lambert, B. et al. Feasibility study on the implementation of a mobile high-resolution PET/CT scanner for surgical specimens: exploring clinical applications and practical considerations. *Eur. J. Nucl. Med. Mol. Imaging* <https://doi.org/10.1007/s00259-025-07143-z> (2025).
20. Garcia, M. T. et al. Accuracy of frozen section in intraoperative margin assessment for breast-conserving surgery: A systematic review and meta-analysis. *PLoS One* **16**, e0248768 (2021).
21. Tan, M. P., Sitoh, N. Y. & Sim, A. S. The value of intraoperative frozen section analysis for margin status in breast conservation surgery in a nontertiary institution. *Int. J. Breast Cancer* **2014**, 715404 (2014).
22. Samson, K. Post-lumpectomy recurrence rates down sharply with treatment advances. *Oncology* **40**, 50 (2018).
23. Di Grezia, G. et al. Reducing costs of breast examination: ultrasound performance and inter-observer variability of expert radiologists versus residents. *Cancer Invest.* **34**, 355–360 (2016).
24. Armani, A. et al. Intraoperative margin trials in breast cancer. *Curr. Breast Cancer Rep.* **14**, 65–74 (2022).
25. Debacker, J. et al. Three-dimensional margin assessment in head and neck malignancies using a submillimetric 18F-FDG PET/CT, results of an ongoing clinical trial. *Oral. Oncol.* **118**, 5 (2021).
26. Muraglia, L. et al. First live-experience session with PET/CT specimen imager: A pilot analysis in prostate cancer and neuroendocrine tumor. *Biomedicines* **11**, 645 (2023).
27. Moraitis, A. et al. Evaluation of surgical margins with intraoperative PSMA PET/CT and their prognostic value in radical prostatectomy. *J. Nucl. Med.* <https://doi.org/10.2967/jnumed.124.268719> (2025).
28. Covington, M. F. et al. PET-CT in clinical adult oncology: II. Primary thoracic and breast malignancies. *Cancers* **14**, 11, 2689, <https://doi.org/10.3390/cancers14112689> (2022).
29. Lester, S. C. et al. Protocol for the examination of specimens from patients with ductal carcinoma in situ of the breast. *Arch. Pathol. Lab Med.* **133**, 15–25 (2009).
30. Lester, S. C. et al. Protocol for the examination of specimens from patients with invasive carcinoma of the breast. *Arch. Pathol. Lab Med.* **133**, 1515–1538 (2009).

Acknowledgements

This work was supported by Innovation mandates grants no. HPC.2016.0240. and HPC.2017.0515 by Agency for Innovation through Science and Technology (IM-IWT).

Author contributions

A.D.C. Assisted with data collection; contributed to the interpretation of the images; performed data analysis; interpreted results; wrote and revised the manuscript. G.V., G.C., P.D.V., K.M., and B.V.B. contributed to the interpretation of the images; reviewed and edited the manuscript. P.T., G.B., R.S., K.V.V., L.V., C.M., J.D., S.H., and H.D. (both Herman Depypere and Hannelore Denys), provided critical insights and theoretical guidance; reviewed and edited the manuscript. M.G. conceived and designed the study; collected and managed data; contributed to the interpretation of the images; provided critical insights and theoretical guidance; reviewed and edited the manuscript. All authors have read and approved the final manuscript and agree with the order of authorship.

Competing interests

The authors declare no competing interests.

Additional information

Supplementary information The online version contains supplementary material available at <https://doi.org/10.1038/s41523-025-00818-8>.

Correspondence and requests for materials should be addressed to Anne-Sofie De Crem or Menekse Göker.

Reprints and permissions information is available at <http://www.nature.com/reprints>

Publisher's note Springer Nature remains neutral with regard to jurisdictional claims in published maps and institutional affiliations.

Open Access This article is licensed under a Creative Commons Attribution-NonCommercial-NoDerivatives 4.0 International License, which permits any non-commercial use, sharing, distribution and reproduction in any medium or format, as long as you give appropriate credit to the original author(s) and the source, provide a link to the Creative Commons licence, and indicate if you modified the licensed material. You do not have permission under this licence to share adapted material derived from this article or parts of it. The images or other third party material in this article are included in the article's Creative Commons licence, unless indicated otherwise in a credit line to the material. If material is not included in the article's Creative Commons licence and your intended use is not permitted by statutory regulation or exceeds the permitted use, you will need to obtain permission directly from the copyright holder. To view a copy of this licence, visit <http://creativecommons.org/licenses/by-nc-nd/4.0/>.

© The Author(s) 2025